Conf-780854--1

LA-UR-78-2325

MASTER

MACROSCOPIC DESCRIPTION OF HEAVY-ION REACTIONS

by

J. Rayford Nix

August 20, 1978

For presentation at the
International Conference on Nuclear Interactions
Canberra, Australia, August 28–September 1, 1978

PREPRINT FROM

los alamos
scientific laboratory
of the University of California
LOS ALAMOS, NEW MEXICO 87545

UNITED STATES
ENERGY RESEARCH AND
DEVELOPMENT ADMINISTRATION
CONTRACT W-7405-ENG. 36

MACROSCOPIC DESCRIPTION OF HEAVY-ION REACTIONS

J. Rayford Nix

Theoretical Division, Los Alamos Scientific Laboratory

University of California, Los Alamos, New Mexico 87545, U.S.A.

Abstract

We discuss the statics and dynamics of large scale nuclear collective motion, with special emphasis on very-heavy-ion reactions. Compound-nucleus cross sections are calculated by use of the criterion that the dynamical trajectory for the fusing system must pass inside the fission saddle point in a multidimensional space in order to form a compound nucleus. In an effort to understand whether nuclear dissipation is dominated by two-body collisions or by the interaction of particles with the mean field generated by the remaining particles, we compare the predictions of various macroscopic approaches with those of time-dependent mean-field (Hartree-Fock) theories.

Introduction

Very-heavy-ion reactions are providing us the opportunity to study large-scale nuclear collective motion for systems that are almost twice as heavy as any known nuclei and for shapes that are far removed from a sphere. This is extending greatly our understanding of nuclear shape changes acquired recently from studies of nuclear fission.

For the description of such large-scale nuclear collective motion, we may use either a microscopic approach or a macroscopic approach. Within the former approach, substantial progress has been made recently in terms of the time-dependent mean-field (Hartree-Fock) approximation [1,2]. I would like to discuss this approximation, which leads to several predictions that are qualitatively different from those of most macroscopic approaches, near the end of my talk.

My main concern here will be with a macroscopic approach, which is based on the relatively large number of degrees of freedom in a heavy nuclear system. In this approach, one starts with a distribution of matter that is subjected to given forces and solves the resulting classical equations of motion in some approximation. Although attempts have been made recently to solve the equations of motion directly by use of finite-difference techniques [3], the more common procedure is to assume that the matter is incompressible and to specify the nuclear shape by means of a small number of collective coordinates. This leads to a system of coupled nonlinear differential equations, whose solution for a given set of initial conditions specifies the time evolution of the nuclear shape [4-7]. This time evolution depends upon three fundamental nuclear properties: (1) the nuclear potential energy of deformation, (2) the collective kinetic energy, and (3) the dissipation mechanism for converting collective energy into internal single-particle excitation energy. The internal degrees of freedom are treated implicitly, in contrast to the explicit treatment of the collective degrees of freedom.

Potential Energy

The nuclear potential energy of deformation consists of a nuclear macroscopic energy, a Coulomb energy, a centrifugal energy, and a single-particle correction. For nuclei with zero internal energy, the last term may be calculated by use of Strutinsky's method [8,9]. This term in general decreases with increasing internal energy.

An example of the nuclear macroscopic energy and Coulomb energy, as well as their sum, is shown in Fig. 1 for the collision of two spherical ^{84}Kr nuclei [10]. The energies are plotted as functions of the distance r between the centers of mass of the two halves of the system, for a specified one-dimensional sequence of shapes. These shapes are generated by assuming that after the nuclei come into contact the density remains constant throughout the shape, with the displaced matter simply filling in the neck region. This is valid only when the relative velocities after contact are small compared to the nuclear speed of sound. At higher incident energies, the increase in density in the neck region would lead to an increase in potential energy as the nuclei come together.

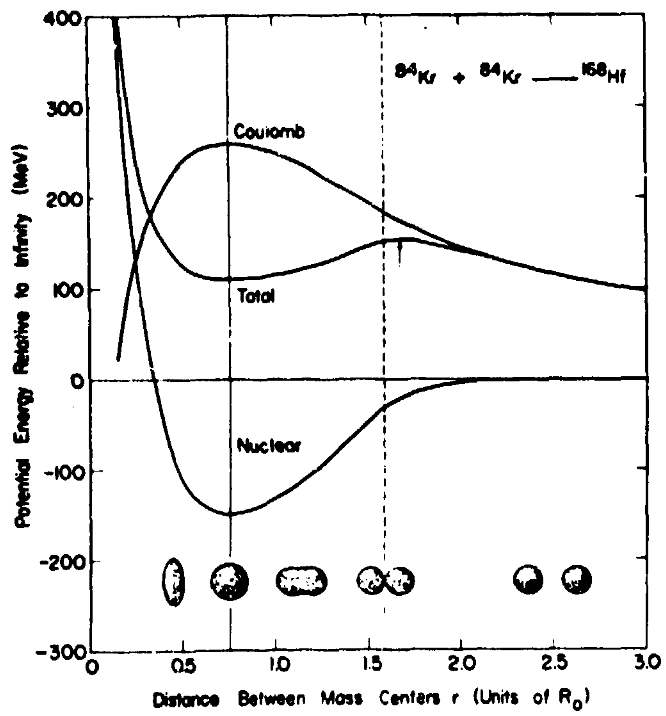

Fig. 1. Nuclear macroscopic energy, Coulomb energy, and their sum for the reaction $^{84}Kr + ^{84}Kr \rightarrow ^{168}Hf$. The energies are plotted as functions of the distance r between the centers of mass of the two halves of the system, in units of the radius R_0 of the spherical compound nucleus ^{168}Hf.

The nuclear macroscopic energy shown in Fig. 1 was calculated by means of a double volume integral of a Yukawa effective two-nucleon interaction [10-13]. This procedure, which suffers from the lack of any aspects of nuclear saturation, leads to nuclear potentials that decrease more slowly with increasing distance than nuclear potentials derived from heavy-ion elastic-scattering data [14,15].

This deficiency may be corrected either by use of the proximity formalism of Swiatecki and coworkers [16], or alternatively by use of an effective two-nucleon interaction that yields a minimum nuclear macroscopic energy for zero separation between two semi-infinite slabs of nuclear matter [17]. By starting with the difference between two Yukawa functions whose strengths are required to reproduce this saturation condition and the correct nuclear surface energy, one finds that the ranges of both Yukawa functions must be approximately equal in order to reproduce heavy-ion elastic-scattering data. In the limit in which the ranges are equal, this new potential is obtained by multiplying the old single-Yukawa potential by the Yukawa range a and differentiating with respect to a, which leads to a Yukawa-plus-exponential effective two-nucleon interaction [17].

For two separated spherical nuclei, the resulting nuclear potential may be written as

$$V_n = -V_{red}\left(2 + \frac{s}{a}\right) e^{-s/a} \quad ,$$

where

$$s = r - (R_1 + R_2)$$

is the separation between the inner surfaces of the two nuclei of equivalent-sharp radii R_1 and R_2, and where a is the range of the Yukawa and exponential functions. The potential reduction factor V_{red} is in general a function of both the nuclear system and the separation s [17]. However, when $R_1/a \gg 1$ and $R_2/a \gg 1$, it simplifies to

$$V_{red} \approx a c_s R_1 R_2 / [r_0^2 (R_1 + R_2)] \quad ,$$

where r_0 is the nuclear-radius constant, whose value is taken from an analysis of electron-scattering data and muonic-atom data [18], and where

$$c_s = a_s \left\{ \left[1 - \kappa_s \left(\frac{N_1 - Z_1}{A_1} \right)^2 \right] \left[1 - \kappa_s \left(\frac{N_2 - Z_2}{A_2} \right)^2 \right] \right\}^{1/2} ,$$

with a_s the surface-energy constant and κ_s the surface-asymmetry constant.

Although at the above level of approximation the Yukawa-plus-exponential potential gives the same result as the proximity formalism [16], when treated exactly it contains geometrical corrections that are somewhat different. For this exact treatment, we compare in Fig. 2 the predictions of the Yukawa-plus-exponential potential with values of the nuclear potential determined experimentally from heavy-ion elastic-scattering data and heavy-ion fusion data [17]. Although some discrepancies are evident, this approach describes the main features of the nuclear potential as determined by these reactions.

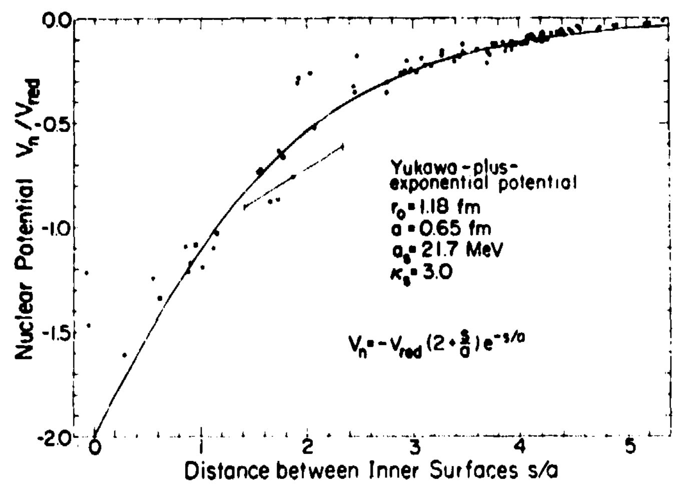

Fig. 2. Comparison of the Yukawa-plus-exponential nuclear potential (solid curve) with values derived from heavy-ion elastic-scattering data (solid points) and heavy-ion fusion data (open points).

In addition to heavy-ion reactions, the Yukawa-plus-exponential potential can be used for fission and nuclear ground-state masses and deformations. As shown in Fig. 3, this approach reproduces the fission barriers of rare-earth nuclei through actinide nuclei to within an accuracy of 1 or 2 MeV [17], when single-particle effects are calculated by use of a folded-Yukawa single-particle potential [19,20]. This approach also reproduces the ground-state masses of 165 even nuclei in the actinide region and four regions of spherical nuclei with a root-mean-square deviation of 1.2 MeV [17].

In both fission and very-heavy-ion reactions, the end portions of the system in general are of unequal size and do not remain spherical. Therefore, in addition to the coordinate r that specifies the distance between the left-hand and right-hand portions of the system, we need a mass-asymmetry coordinate α and a fragment-elongation coordinate σ. The former is defined as the difference in mass between the two portions, divided by the total mass, and the latter is defined as the sum of the root-mean-square extensions along the symmetry axis of the mass of each portion about its center of mass [12,13]. Of course, for a shape without a well-defined neck, some prescription must be adopted for dividing the system into two portions [13].

We show in Fig. 4 some of the nuclear shapes corresponding to various values of r and σ, when the mass asymmetry $\alpha = 0$ [12]. The lower left-hand part of the figure corresponds

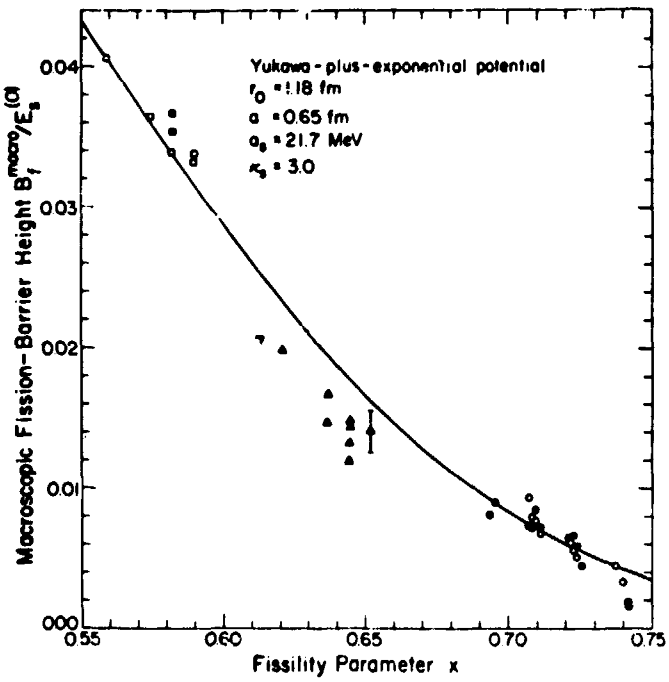

Fig. 3. Comparison of the Yukawa-plus-exponential fission-barrier height (solid curve) with the macroscopic contributions to experimental fission-barrier heights (points).

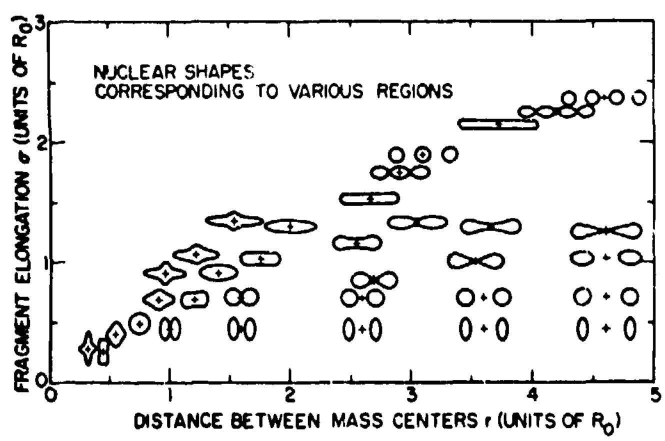

Fig. 4. Nuclear shapes corresponding to various values of r and σ, which are indicated by plus signs.

to a single composite system, and the lower right-hand part corresponds to two separated nuclei. Extending diagonally toward the upper right-hand corner are three-fragment and four-fragment configurations, which are separated from each other by elongated cylinder-like shapes.

Figure 5 shows as a function of these two coordinates the macroscopic potential energy for head-on collisions in the reaction $^{110}Pd + ^{110}Pd \rightarrow ^{220}U$, calculated with the single-Yukawa potential [12]. The binary fission saddle point, whose location is indicated by two short crossed lines, lies 6.3 MeV higher in energy than the spherical ^{220}U nucleus, whose location is indicated by a single solid dot. The point of first contact in heavy-ion reactions, whose location is indicated by two adjacent solid dots, lies some 24 MeV higher in

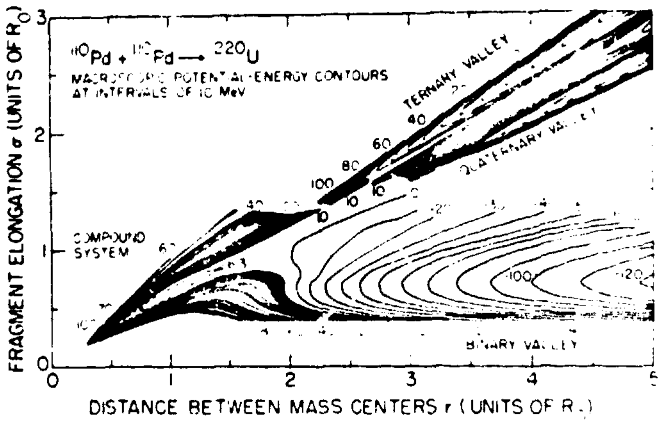

Fig. 5. Macroscopic potential-energy contours for the ^{220}U nuclear system, in units of MeV.

energy than the binary saddle point. In this two-dimensional space, the path between the contact point and the sphere is on the side of a steep hill, with the potential energy decreasing rapidly toward increasing fragment elongation σ.

For nuclear systems lighter than about ^{220}U the macroscopic zero-angular-momentum binary saddle point lies outside the contact point, which permits compound-nucleus formation to occur whenever the ions are brought into contact at moderate energies. However, for nuclear systems heavier than about ^{220}U, the macroscopic zero-angular-momentum binary saddle point lies inside the contact point, with its location moving toward the sphere as the size of the system increases [12].

Nuclear Dynamics

A necessary condition for forming a compound nucleus is that the dynamical trajectory for the fusing system pass inside the fission saddle point in a multidimensional space [6]. In addition to the potential energy, the dynamical trajectory depends upon the collective kinetic energy and the mechanism of nuclear dissipation.

We calculate the collective kinetic energy for nuclear flow that is a superposition of incompressible, nearly irrotational collective-shape motion and rigid-body rotation [4-7]. As an approximation to irrotational flow we use the Werner-Wheeler method, which determines the flow in terms of circular layers of fluid [4,5]. Angular momentum is taken into account approximately by means of a pseudopotential that is calculated for the rigid-body rotation of nuclear shapes that are required to remain axially symmetric about an axis that is rotating in space [6]. The nuclear shapes are described in terms of smoothly joined portions of three quadratic surfaces of revolution [4].

Nuclear dissipation is included by means of the Rayleigh dissipation function [5,7,9], which depends upon the nuclear shape and time rate of change of the shape, as well as upon the particular mechanism that is used for converting collective energy into internal energy. At present we know very little about this mechanism, but are exploring possibilities that range from ordinary two-body viscosity, which arises from the collision of nucleons with each other [5], to one-body dissipation, which arises from the collision of nucleons with the moving nuclear surface [7,21].

The resulting generalized Lagrange equations of motion are transformed into the generalized Hamilton equations of motion and integrated numerically to determine the dynamical trajectory, for a given set of initial conditions. For the case in which the nuclear dissipation is zero, we show in Fig. 6 some examples of these trajectories for the reaction ^{110}Pd + ^{110}Pd → ^{220}U at a bombarding energy in the center-of-mass system that is 20 MeV above the maximum in the one-dimensional zero-angular-momentum interaction barrier [6]. At this bombarding energy, only those trajectories with angular momentum ℓ less than the critical value $\ell_{crit} = 45$ pass inside the fission saddle point for that angular momentum (indicated by the points) and lead to compound-nucleus formation.

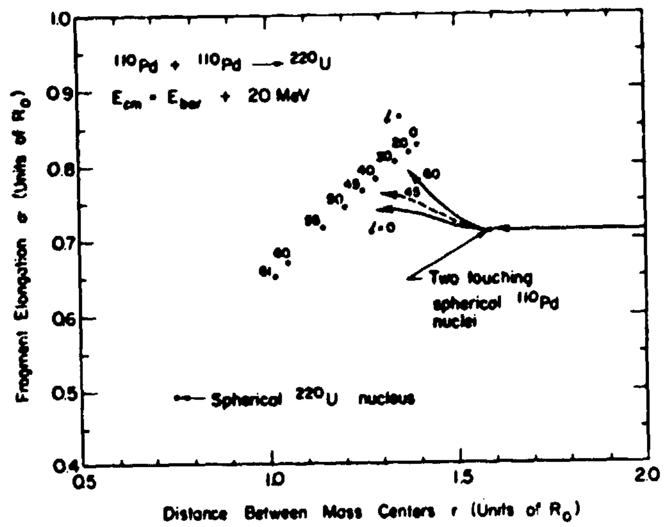

Fig. 6. Dynamical trajectories for the reaction $^{110}Pd + ^{110}Pd \rightarrow ^{220}U$.

The resulting compound-nucleus cross section for this system is shown by the solid curve in Fig. 7 [6]. In the energy region below the arrow in the solid curve, the compound-nucleus cross section is determined by the requirement that the dynamical trajectory pass inside the fission saddle point. This requirement reduces substantially the compound-nucleus cross section compared to that calculated for a one-dimensional interaction barrier, which is shown by the dashed curve. In the energy region above the arrow in the solid curve, the compound-nucleus cross section is determined by the angular momentum at which the fission saddle point disappears.

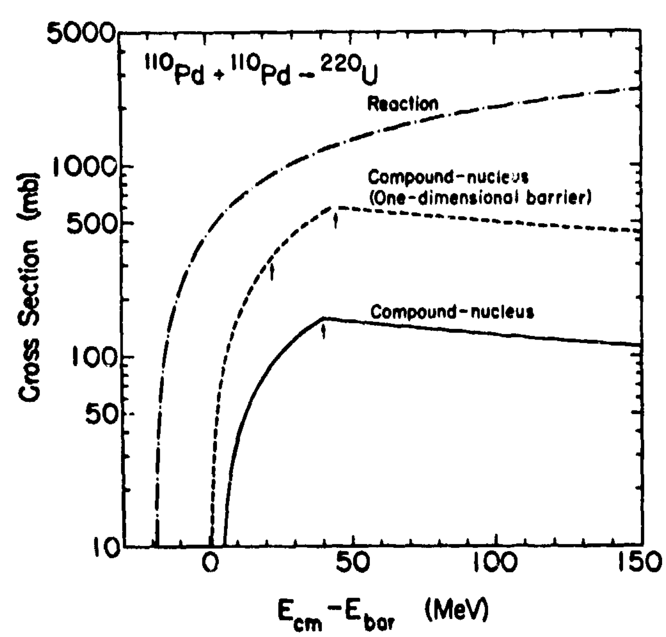

Fig. 7. Comparison of various cross sections for the reaction $^{110}Pd + ^{110}Pd \rightarrow ^{220}U$. The results are plotted as functions of the center-of-mass bombarding energy relative to the maximum in the one-dimensional zero-angular-momentum interaction barrier.

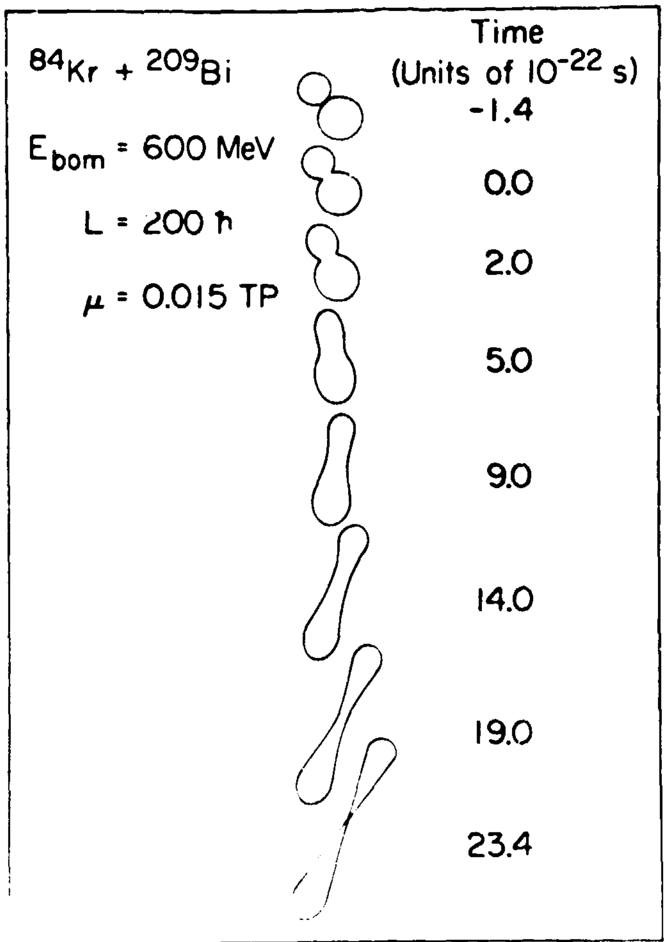

Fig. 8. Time evolution of the nuclear shape for the reaction ^{84}Kr + ^{209}Bi, calculated for a two-body viscosity coefficient $\mu = 0.015$ TP $= 9 \times 10^{-24}$ MeV s/fm^3 . The laboratory bombarding energy is 600 MeV, and the angular momentum is 200 ħ .

As shown by the dot-dashed curve, the total reaction cross section, which is determined by the point at which the tails of the two nuclear densities begin to overlap rather than by the subsequent dynamical motion, is roughly 10 times the compound-nucleus cross section. As the size of the nuclear system increases, the fission saddle point moves toward the sphere, which decreases the compound-nucleus cross section.

For the case in which the nuclear dissipation proceeds by ordinary two-body viscosity, we show in Fig. 8 a calculation of a highly inelastic collision [22]. After the ^{84}Kr and ^{209}Bi nuclei come into contact, the system develops an appreciable neck, which is followed by a substantial elongation of the two portions of the system. The initial bombarding energy is therefore converted partly into collective potential and kinetic energy, and partly into internal single-particle excitation energy.

For a given angular momentum, such calculations predict the most probable final kinetic energies, angles, and masses of the fragments emerging from a heavy-ion collision. In addition to the most probable values, the widths of the distributions in these quantities are also important. These widths arise partly from quantal fluctuations that give rise to distributions in the values of the initial collective coordinates and their conjugate momenta [4,23] and partly from neglecting the effect of the internal coordinates on the dynamical path. Through the introduction of an effective diffusion constant, this latter effect is often assumed to be responsible for the entire widths of the distributions in the final quantities of interest [24-26].

Comparison with Mean-Field Theories

I would like now to turn to a microscopic approach for the description of large-scale nuclear collective motion. The ultimate microscopic approach--nirvana--would consist of a quantal relativistic time-dependent many-body theory with all hadronic degrees of freedom included. Of course, in order to reduce such an ultimate theory to something that is tractable, we must make several approximations [27].

First, we must specify which degrees of freedom are to be treated explicitly (for example, only the nucleons) and which implicitly. Second, we must give up relativity, which leads to a time-dependent many-body Schrödinger equation. Third, we must approximate the time-dependent many-body wave function in some way. Although we could attempt to take into account correlations between the particles by use of a correlated wave function, in practice it is necessary to introduce an effective interaction, at which stage an approximate generator-coordinate wave function could be used. If, finally, there are many degrees of freedom and no explicit correlations, we are led to an independent-particle wave function, such as a time-dependent Hartree-Fock wave function.

Such mean-field theories have been used recently to calculate what happens in both heavy-ion reactions [1] and in fission [2], with some predictions that are qualitatively different from those of most macroscopic approaches. As an example, we show in Fig. 9 the

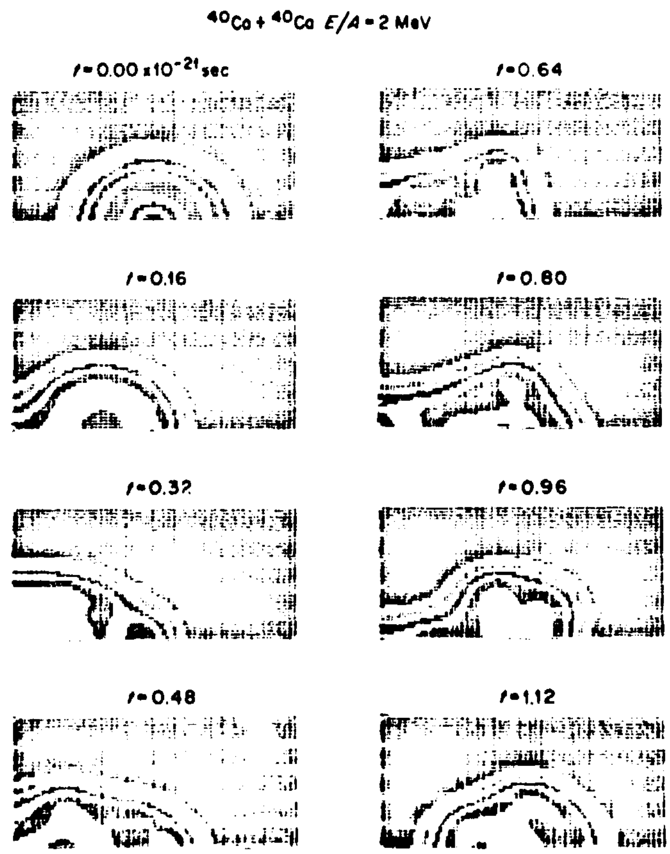

Fig. 9. Time evolution of the nuclear density for the head-on collision of ^{40}Ca + ^{40}Ca, calculated with the time-dependent Hartree-Fock approximation. The center-of-mass bombarding energy per compound nucleon is 2 MeV, which corresponds to a laboratory bombarding energy per projectile nucleon of 8 MeV.

results calculated in the time-dependent Hartree-Fock approximation for the head-on collision of two ^{40}Ca nuclei at a laboratory bombarding energy of 320 MeV [1]. Because in this approximation the particles interact only with the mean field generated by the remaining particles, the two nuclei pass through each other rather than forming a compound nucleus. During this interpenetration, the composite system maintains a prolate shape. By way of contrast, in most macroscopic approaches the system would proceed from an initially prolate shape to an oblate shape, then undergo damped oscillations about the spherical shape, and finally form a compound nucleus. Some attempts have been made recently to extend the time-dependent Hartree-Fock approximation by taking into account two-body collisions [28,29].

As a final example, we compare in Fig. 10 the results calculated with the time-dependent Hartree-Fock approximation for the fission of ^{236}U with those calculated with four different macroscopic approaches [2]. The time-dependent Hartree-Fock calculations are performed for shapes that are reflection-symmetric and axially symmetric, for a constant pairing gap of 2 MeV that is designed to simulate the effects of deviations from symmetric shapes, and for zero spin-orbit interaction. The four macroscopic calculations are performed for zero dissipation, for ordinary two-body viscosity, and for two versions of one-body dissipation. The results of the time-dependent Hartree-Fock calculation are qualitatively similar to those of the first three macroscopic approaches. Unfortunately, it is not possible from this comparison to distinguish between such drastically different mechanisms for nuclear dissipation as two-body viscosity and one version of one-body dissipation.

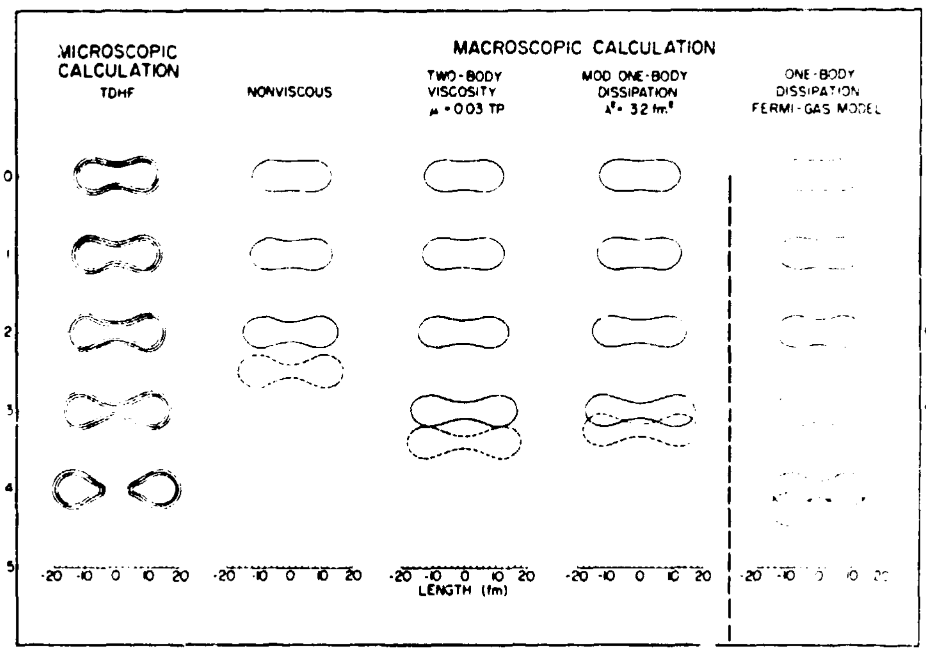

Fig. 10. Time evolution of the nuclear shape for the fission of ^{236}U, calculated with the time-dependent Hartree-Fock approximation and with four different macroscopic approaches. In each case the initial conditions correspond to starting from rest at a point beyond the fission saddle point that is 1 MeV lower in energy than the saddle-point energy.

Outlook

By means of very-heavy-ion reactions, we are now embarking on a study of the dynamics of large-scale nuclear collective motion. As is true with any field in its infancy, many important questions remain to be answered. Are nuclei more nearly mobile like water, or more nearly viscous like honey? Do nuclei dissipate their collective energy primarily through collisions between individual particles, or through collisions of particles with the moving nuclear surface? Do the many approximations that are necessary to reduce the ultimate microscopic theory to something that is tractable invalidate the predictions of mean-field theories? Are we able to obtain a satisfactory macroscopic description?

Some of these questions will be answered ultimately through comparisons with experimental data obtained by continuing to bombard various targets with various projectiles at various energies. However, some of the more important ones could be answered much sooner by performing experiments that are carefully designed to test the unique predictions of the mean-field theories and various macroscopic approaches. I hope that some of the experimentalists in the audience will rise to the challenge!

Acknowledgments

I am grateful to H. J. Krappe and A. J. Sierk for their collaboration on the studies that led to Figs. 2 and 3. This work was supported by the United States Department of Energy

References

1. Koonin, S. E., K. T. R. Davies, V. Maruhn-Rezwani, H. Feldmeier, S. J. Krieger, and J. W. Negele, 1977. Phys. Rev. C 15:1359-1374.
2. Negele, J. W., S. E. Koonin, P. Möller, J. R. Nix, and A. J. Sierk, 1978. Phys. Rev. C 17:1098-1115.
3. Alonso, C. T., 1976. *Proc. Int. Col. on Drops and Bubbles*, Pasadena, California, 1974 (California Institute of Technology, Pasadena), Vol. I, pp. 139-157.
4. Nix, J. R., 1969. Nucl. Phys. A130:241-292.
5. Davies, K. T. R., A. J. Sierk, and J. R. Nix, 1976. Phys. Rev. C 13:2385-2403.
6. Nix, J. R., and A. J. Sierk, 1977. Phys. Rev. C 15:2072-2082.
7. Sierk, A. J., S. E. Koonin, and J. R. Nix, 1978. Phys. Rev. C 17:646-653.
8. Brack, M., J. Damgaard, A. S. Jensen, H. C. Pauli, V. M. Strutinsky, and C. Y. Wong, 1972. Rev. Mod. Phys. 44:320-405.
9. Nix, J. R., 1972. Ann. Rev. Nucl. Sci. 22:65-120.
10. Nix, J. R., and A. J. Sierk, 1974. Phys. Scr. 10A:94-100.
11. Krappe, H. J., and J. R. Nix, 1974. *Proc. Third IAEA Symp. on the Physics and Chemistry of Fission*, Rochester, New York, 1973 (IAEA, Vienna), Vol. I, pp. 159-176.
12. Möller, P., and J. R. Nix, 1976. Nucl. Phys. A272:502-532.
13. Möller, P., and J. R. Nix, 1977. Nucl. Phys. A281:354-372.
14. Zint, P. G., and U. Mosel, 1976. Phys. Rev. C 14:1488-1498.
15. Sierk, A. J., 1977. *Proc. Symp. on Heavy-Ion Elastic Scattering*, Rochester, New York, 1977, University of Rochester Report, pp. 306-320.
16. Błocki, J., J. Randrup, W. J. Swiatecki, and C. F. Tsang, 1977. Ann. Phys. (N.Y.) 105:427-462.
17. Krappe, H. J., J. R. Nix, and A. J. Sierk, 1978. Los Alamos Scientific Laboratory Preprint No. LA-UR-78-2289, pp. 1-14.
18. Myers, W. D., 1976. At. Data Nucl. Data Tables 17:411-417.
19. Möller, P., and J. R. Nix, 1974. Nucl. Phys. A229:269-291.
20. Möller, P., S. G. Nilsson, and J. R. Nix, 1974. Nucl. Phys. A229:292-319.
21. Błocki, J., Y. Boneh, J. R. Nix, J. Randrup, M. Robel, A. J. Sierk, and W. J. Swiatecki, 1978. Ann. Phys. (N.Y.), to be published.
22. Sierk, A. J., and J. R. Nix, 1976. *Proc. Symp. on Macroscopic Features of Heavy-Ion Collisions*, Argonne, Illinois, 1976, Argonne National Laboratory Report No. ANL/PHY-76-2, Vol. I, pp. 407-429.
23. Esbensen, H., A. Winther, R. A. Broglia, and C. H. Dasso, 1978. Niels Bohr Institute Preprint, pp. 1-10.
24. Nörenberg, W., 1974. Phys. Lett. 52B:289-292.
25. Moretto, L. G., and J. S. Sventek, 1975. Phys. Lett. 58B:26-30.
26. Agassi, D., H. A. Weidenmüller, and G. Mantzouranis, 1975. Phys. Rep. 22C:145-179.
27. Amsden, A. A., F. H. Harlow, and J. R. Nix, 1977. Phys. Rev. C 15:2059-2071.
28. Wong, C. Y., and H. H. K. Tang, 1978. Phys. Rev. Lett. 40:1070-1073.
29. Orland, H., and R. Schaeffer, 1978. C. E. N. Saclay Preprint No. DPh-T/78/41, pp. 1-37.